Bioorganic & Medicinal Chemistry 19 (2011) 2218–2230

Contents lists available at ScienceDirect

Bioorganic & Medicinal Chemistry

journal homepage: www.elsevier.com/locate/bmc

CyDEPMPOs: A class of stable cyclic DEPMPO derivatives with improved properties as mechanistic markers of stereoselective hydroxyl radical adduct formation in biological systems

Gaëlle Gosset [a], Jean-Louis Clément [a], Marcel Culcasi [a,*], Antal Rockenbauer [b], Sylvia Pietri [a]

[a] Sondes Moléculaires en Biologie, Laboratoire Chimie Provence, CNRS UMR 6264, Universités d'Aix-Marseille, Centre Scientifique de Saint-Jérôme (Case 522), 13397 Marseille Cedex 20, France
[b] Chemical Research Center, Institute of Structural Chemistry, Budapest, Hungary

ARTICLE INFO

Article history:
Received 21 December 2010
Revised 14 February 2011
Accepted 18 February 2011
Available online 26 February 2011

Keywords:
ESR
Spin trapping
DEPMPO
Hydroxyl radical
Diastereoisomeric spin adducts

ABSTRACT

The *cis/trans* diastereoisomeric composition of hydroxyl radical adducts to chiral cyclic nitrones can be used to approach mechanisms of free radical formation in biological systems. Such determination is greatly simplified when both diastereoisomers have ESR spectra with at least two non-overlapping lines. To achieve this prerequisite, a series of DEPMPO-derived spin traps bearing one unsubstituted or alkyl-substituted 2-oxo-1,3,2-dioxaphosphorinane ring were synthesized and their structures were confirmed by X-ray diffraction, ^{1}H, ^{13}C and ^{31}P NMR. These CyDEPMPOs nitrones showed variable lipophilicities and LD_{50} values on murine fibroblasts compatible with a safe use in biological spin trapping. All CyDEPMPOs formed persistent spin adducts with a series of free radicals, including superoxide and hydroxyl (i.e., CyDEPMPOs-OH) and the in vitro half-life times of these two latter were at least as extended as those of parent DEPMPO. Using four methods of CyDEPMPOs-OH formation, the *cis*-CyDEPMPOs-OH percentage was found significantly varied with substitution on the P-containing ring and, more interestingly, with the generating system.

1. Introduction

Because superoxide ($O_2^{\cdot-}$) is a key radical species involved in many biological processes, improving its detection conditions in aqueous media using electron spin resonance (ESR) spectrometry has attracted many research groups over the last three decades. Since the pioneering work of Harbour et al.[1] who first reported the ESR spectrum of DMPO-OOH, the protonated $O_2^{\cdot-}$ spin adduct on 5,5-dimethyl-1-pyrroline N-oxide (DMPO; Fig. 1A) in water, synthetic efforts almost uniquely concentrated on the development of DMPO-derived, five-membered ring cyclic nitrones that could form long-lived nitrone-OOH adducts. In this stability regard, a decisive step was achieved by introducing an electron-withdrawing group such as $-P(O)(OEt)_2$, $-CO_2Et$ or $-CONH_2$ at the C-5 position of the DMPO cycle, leading to the 5-diethoxyphosphoryl-5-methyl-1-pyrroline N-oxide (DEPMPO), 5-ethoxycarbonyl-5-methyl-1-pyrroline N-oxide (EMPO) and AMPO families, respectively (Fig. 1A).[2–4] Due to the existence of a strong stabilizing anomeric effect, increased nitrone-OOH half-lives were reported in vitro with derivatives of DEPMPO,[5–13] EMPO[14–21] or AMPO,[22,23] which significantly exceeded that of DMPO-OOH. Thus, using the same experimental conditions for $O_2^{\cdot-}$ generation, the half-life time was ~15 min for DEPMPO-OOH[2] and only ~1 min for DMPO-OOH.[2,24] Despite these advances, in vivo detection of $O_2^{\cdot-}$ still remains limited to reductant-free aqueous media (e.g., re-suspended cells[25] or sub-cellular cell components[11,26] in phosphate-based buffers, or isolated organ perfusates[2]) because of the poor stability of nitrone-OOH in biological fluids such as blood or plasma. Recently destructive bioreduction of nitrone-OOH has been spectacularly slowered, for example, by using β-cyclodextrins either to form inclusion complexes[27,28] or as a framework of derivatized cyclic nitrones.[13,29,30] However, further use of these sophisticated spin traps in small living animals under oxidant stress, ideally combined with low-frequency ESR detection, would require gram scale quantities and toxicity data to be available.

When it does not lead to the total suppression of the ESR signal (e.g., in the presence of ascorbate where the diamagnetic *N*-hydroxylamine is ultimately formed), bioreduction of nitrone-OOH may result in the formation of nitrone-OH, the hydroxyl radical ($HO^{\cdot}$) spin adduct. In the DEPMPO and EMPO series, this mechanism has been observed in vitro with glutathione peroxidase (GPx),[2,3] an enzyme found in cytosol, mitochondria and biological fluids, which converts hydroperoxides into alcohols. Since in oxygenated medium nitrone-OH can also be formed by metal ion-catalyzed nucleophilic addition of water,[2,24,31] this spin adduct

* Corresponding author. Tel.: +33 491289 025; fax: +33 491 288 758.
E-mail address: marcel.culcasi@univ-provence.fr (M. Culcasi).

0968-0896/$ - see front matter © 2011 Elsevier Ltd. All rights reserved.
doi:10.1016/j.bmc.2011.02.040

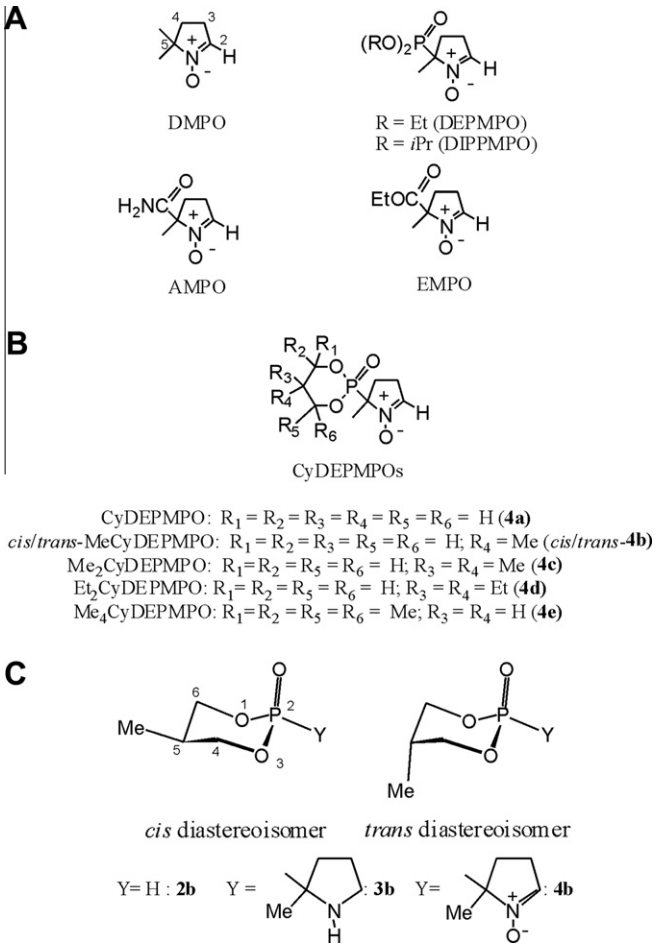

Figure 1. (A) Structure of cyclic nitrones designed for biological spin trapping; (B) structure of CyDEPMPOs; (C) *cis*/*trans* diastereoisomery in the preferred configuration of the 5-methyl-2-oxo-1,3,2-dioxaphosphorinane framework.

is quite often detected in biological spin trapping experiments involving pyrroline N-oxides and thus cannot be considered as a reliable marker of a biologically-relevant HO· formation, for example, by a Fenton-like mechanism involving primary $O_2^{\cdot-}$ generation followed by its dismutation into hydrogen peroxide (H_2O_2). In a recent study,[32] we showed that these three above-mentioned mechanisms of nitrone-OH formation can be discriminated through the ESR analysis of *cis*/*trans* diastereoisomers of DEPMPO-OH, being stereoselectively formed as a result of the presence of a chiral center at C-5 of the nitrone (see Fig. 2 with Y = OH). Whereas this allowed to demonstrate that the HO· adduct signal detected in the effluents of DEPMPO-reperfused isolated rat livers resulted from primary $O_2^{\cdot-}$ formation, *cis*/*trans* analysis required accurate simulation of the two overlapping ESR components of DEPMPO-OH.[32] To improve the reliability of the *cis*/*trans* content in the diastereoisomer method, DEPMPO derivatives having non-overlapping HO· adduct spectra (a common feature in EMPO[3,14,16–21] and AMPO[4,22,23] families) would thus be more suitable. Indeed this unique property

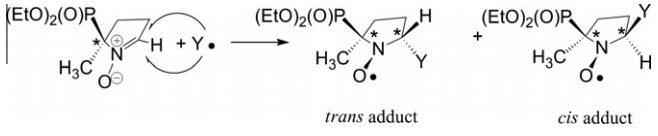

Figure 2. Diastereoisomers formed upon spin trapping on DEPMPO. *Cis*/*trans* positions of Y ligand are relative to the diethoxyphosphoryl substituent.

was reported for the C_5-substituted phenyl DEPMPO[5] but this nitrone showed toxicity upon perfusion in normoxic isolated rat hearts (unpublished results). More recently, a DEPMPO derivative in which the P-atom at C-5 is part of a six-membered ring (i.e., 2-oxo-1,3,2-dioxaphosphorinane) was reported to yield two ESR distinguishable HO· adducts[10] but this behaviour was not further investigated. In the present paper, we describe the spin trapping properties of an extended series of such cyclic DEPMPO analogues (CyDEPMPOs; Fig. 1B) towards a series of different free radicals. We particularly focused on the diastereoisomeric content of their HO· adducts obtained using different generators and propose two of the new nitrones as improved non-toxic spin traps for mechanistic purpose in the study of biological free radicals.

2. Results and discussion

2.1. Synthesis

As first introduced in,[10] we kept CyDEPMPOs as a general acronym of cyclic DEPMPO analogues described herein but with slight modification indicating the nature and number of substituents in the P-containing ring (Fig. 1B).

Synthetic methods used for the preparation of CyDEPMPOs are shown in Scheme 1. The 2-oxo-1,3,2-dioxaphosphinanes **2a**–**2e** were obtained in quantitative yields by modifying the method of Page et al.[33] The critical step of the one-pot synthesis involved addition of 1 equiv of the corresponding 1,3-diol (**1a**–**1e**) in THF. Due to the known anancomeric configurational isomerism at phosphorus in six-membered ring phosphonates,[34] the presence of a single Me at C-5 in the ring of **2b** led to a mixture of *cis*/*trans* diastereoisomers with respect to the preferential axial orientation of the phosphoryl oxygen (Fig. 1C). In this mixture, when homonuclear decoupling of each Me at C-5 was performed at either 454.87 or 582.83 Hz, the H-6 signal in the ^{1}H NMR spectrum (500 MHz in $CDCl_3$) appeared as a triplet of triplets for the major diastereoisomer (66%; $^3J_{5ax,6ax}$ = 11.0 Hz and $^3J_{5ax,6eq}$ = 4.3 Hz) while it was a doublet of triplets of triplets for the minor diastereoisomer (34%; $^3J_{5eq,6ax}$ = 6.6 Hz; $^3J_{5eq,6eq}$ = 3.6 Hz and $^4J_{P,5eq}$ = 1.5 Hz). The largest H-5/H-6 coupling appearing in the major diastereoisomer of **2b**, indicates an axial–axial orientation for H-5 and H-6 such as in *cis*-**2b**.

The α-aminophosphonates **3a**–**3e** were obtained as solids from the corresponding cyclic phosphites **2a**–**2e** by the previously described[35] method involving 2-methyl-1-pyrroline in toluene at room temperature. The *cis*/*trans*-**2b** mixture, which degraded upon tentative chromatographic separation, was directly reacted with 2-methyl-1-pyrroline, yielding *cis*/*trans* diastereoisomers of **3b** which could be separated by column chromatography. From the X-ray crystal structure of **3b** (data to be published elsewhere) a

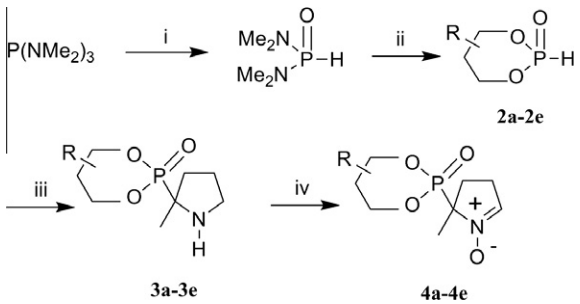

Scheme 1. General synthesis of CyDEPMPOs. Reagents and conditions: (i) 1 equiv H_2O, 3 h, 70 °C, THF; (ii) 1 equiv diol (**1a–1e**), 5 h, 70 °C, THF; (iii) 1.1 equiv 2-methyl-1-pyrroline, 4–6 h, rt, toluene; (iv) 2.1 equiv H_2O_2, 5% Na_2WO_4, 48 h, 0 °C, H_2O.

Table 1
Selected crystallographic data of CyDEPMPOs[a]

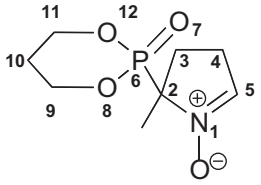

Compound	Bond lengths (Å)			Dihedral angles (°)			
	N(1)–C(5)	C(2)–P(6)	P(6)–O(7)	N(1)C(2)P(6)O(7)	C(5)N(1)C(2)C(3)	P(6)O(8)C(9)C(10)	O(12)P(6)O(8)C(9)
4a	1.301(6)	1.839(4)	1.464(3)	163.9(3)	−13.2(4)	−44.1(5)	22.3(3)
cis-**4b**	1.295(4)	1.832(3)	1.461(2)	48.6(2)	14.7(3)	43.1(3)	−30.9(2)
trans-**4b**	1.285(3)	1.813(2)	1.465(17)	−163.86(14)	−8.1(2)	46.8(2)	−23.97(16)
4c	1.284(4)	1.836(2)	1.459(16)	164.41(15)	15.3(3)	−49.9(2)	25.47(17)
4d	1.282(4)	1.831(3)	1.457(2)	−177.52(18)	−16.53(3)	28.40(3)	−7.7(2)
4e	1.286(4)	1.830(2)	1.457(2)	164.51(18)	12.8(3)	19.5(3)	−6.50(2)

[a] Values in parentheses are the estimated standard deviations.

trans configuration was found for the major diastereoisomer (65% of the mixture; Fig. 1C).

Nitrones **4a**–**4e** were finally obtained from the corresponding compounds **3a**–**3e** by a slow addition of H_2O_2 in the presence of 5% Na_2WO_4 using water as the solvent instead of methanol as reported.[36] After purification by column chromatography and recrystallization chemical structures of nitrones were fully characterized by NMR (^1H, ^{13}C and ^{31}P).

2.2. X-ray crystal structure analysis of nitrones

Selected crystal parameters for CyDEPMPOs are given in Table 1 and ORTEP drawings[37] with 40% probability displacement thermal ellipsoids for nitrones *cis*-**4b**, **4d** and **4e** are shown in Figure 3. The pyrroline ring adopts an envelope conformation having either a E_3 (compounds *cis*-**4b**, **4c**–**4e**) or a ^3E (compounds **4a** and *trans*-**4b**) form as shown by the signs of the C(5)N(1)C(2)C(3) dihedral angles, leaving the C–P bond in an axial or pseudo-equatorial geometry, respectively. Despite its bulkiness the six-membered phosphinane ring is oriented over the nitronyl ring in all nitrones, even the over-crowded **4d** and **4e** (as shown by N(1)C(2)P(6)O(7) dihedral angles close to 180°), with the surprising exception of *cis*-**4b** where the free radical trapping site appears much less sterically hindered (Fig. 3). Taken together these data suggest there may be differences in the spin trapping properties of CyDEPMPOs in biological milieu (in particular *cis*/*trans* ratio) although importance of solvation in water should be considered.

2.3. Lipophilicity and cytotoxicity of nitrones

The 1-octanol/water partition coefficient *P* is an accepted parameter to model membrane penetration, a higher value indicating increased lipophilicity of the molecule (a favorable feature for a spin trap to investigate free radical formation in cell membranes). With respect to DEPMPO, a significant increase in the *P* value was only obtained in the most substituted CyDEPMPOs, i.e., Me_4CyDEPMPO and Et_2CyDEPMPO (Table 2), this latter nitrone being even more lipophilic than 5-diisopropoxyphosphoryl-5-methyl-1-pyrroline N-oxide (DIPPMPO, see structure in Fig. 1A). In the DEPMPO family a dramatic increase of *P* has been reported (i) with increasing the length of the alkyl chain attached to phosphorus,[6] or (ii) in 5-phenylated substituents.[5,8]

In this study, incubation of 3T3 cells with 50 mM of selected nitrones variably affected membrane integrity, as characterized by cellular LDH release (an indicator of cytotoxicity), and LD_{50} and LD_{10} values were determined from dose–response experiments (up to 0.1 M; Table 2). Compared to the acyclic *N*-*t*-butyl-α-phenylnitrone (PBN), the by far more lipophilic and toxic tested

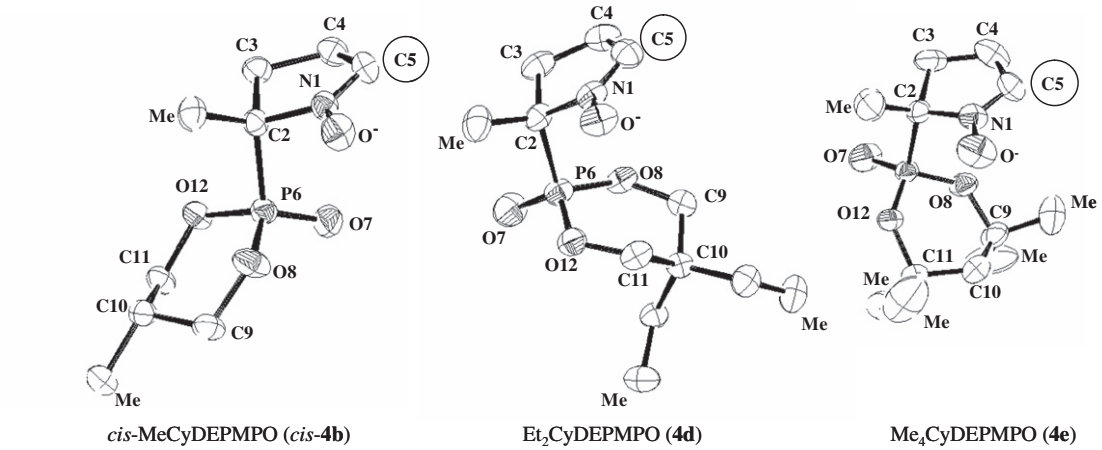

cis-MeCyDEPMPO (*cis*-**4b**) Et_2CyDEPMPO (**4d**) Me_4CyDEPMPO (**4e**)

Figure 3. ORTEP drawings of nitrones *cis*-**4b**, **4d** and **4e** showing the labelling of non-H atoms and their displacement ellipsoids at the 40% probability level. Free radical addition occurs at C-5 (encircled).

Table 2
n-Octanol/water partition coefficients *P*, molar absorptivity ε and in vitro cell toxicity data of nitrones

Compound	*P*[a]	ε[b] (L mol^{-1} cm^{-1})	LDH release[c] (IU/L)	LD_{50} (LD_{10})[d] (mM)
CyDEPMPO	0.04 ± 0.03	8050	7.6 ± 1.8*	122
trans-MeCyDEPMPO	0.10 ± 0.01	8306	nm	nm
cis-MeCyDEPMPO	0.10 ± 0.01	7849	nm	nm
Me_2CyDEPMPO	0.14 ± 0.01[e]	8260	12.5 ± 4.0	112
Et_2CyDEPMPO	1.03 ± 0.04	8020	25.6 ± 3.7*	55 (31)
Me_4CyDEPMPO	0.23 ± 0.01	7992	15.7 ± 5.9	93 (68)
DEPMPO	0.17 ± 0.01[e]	8168	6.4 ± 0.9*	129
DIPPMPO	0.80 ± 0.09[e]	7500	38.9 ± 6.1*	49 (25)
EMPO	0.19 ± 0.04[e]	7807	11.7 ± 2.7	118
PBN	15.1 ± 0.76	17671	79.4 ± 13.5*	7

nm, not measured.
[a] Mean value ± SD ($n \geqslant 4$).
[b] Measured at λ_{max} = 234 nm.
[c] LDH release was measured after 24 h incubation with 50 mM of each spin trap. Values are mean ± SD (n = 6–12). In untreated 3T3 cells baseline LDH release was 12.7 ± 1.9 IU/L. Statistics: *p <0.01 versus untreated cells.
[d] LD_{50} and LD_{10}, the concentrations leading to 50% and 10% cell death, respectively, were determined using the neutral red assay from dose–response experiments after 24 h incubation with each spin trap. Values are mean ± SD (n = 3).
[e] Previously reported data were: Me_2CyDEPMPO, 0.11;[10] DEPMPO, 0.1;[6] DIPPMPO, 2.1[7] and EMPO, 0.1.[17]

compound, cyclic nitrones were significantly better tolerated by the cells, the more lipophilic compounds (i.e., Et_2CyDEPMPO and DIPPMPO) however showing a moderate toxicity. A high spin trap lipophilicity, by facilitating subcellular distribution,[38] could be an important property in the design of specific anti-free radical protectors but there have been many controversial examples in cell studies on PBN[39,40] and some EMPO derivatives[41,42] where a high *P* value was associated with strong intrinsic cytotoxicity at high concentrations. With the aim to evidence spin adduct formation in biological systems under oxidative stress using ESR detection, LD_{50} and LD_{10} data of Table 2 suggest that a safe CyDEPMPOs concentration would be at least 30–50 mM. We previously evidenced the particular involvement of the phosphonate group in the hemodynamic protection against cardiac reperfusion provided by DEPMPO and its pyrrolidine analogue.[43] Thus, a similar property could explain why DEPMPO and all CyDEPMPOs except Et_2CyDEPMPO could decrease LDH release of untreated cells. In this regard additional mechanisms are possible: (i) scavenging on the nitronyl group of radicals produced under usual hyperoxic conditions of cell culture, as postulated for EMPO-type nitrones,[41,42] and/or (ii) a known[44] pharmacological effect of a number of prodrugs containing the P-containing heterocyle of CyDEPMPOs, which is also present in cyclic adenosine monophosphate.

2.4. Superoxide and *tert*-butoxyl radical adducts

Although the design of spin traps having $O_2^{\cdot-}$ adducts with better stabilities than available nitrones was not the purpose of this study, it was nevertheless expected the resulting CyDEPMPOs-OOH nitroxides would present ESR features and half-life times close to that of parent DEPMPO-OOH (i.e., ~11–15 min at pH ~7[2,6,9]). Generation of $O_2^{\cdot-}$ or *t*BuOO$^{\cdot}$ in the presence of **4a**–**4e** yielded the ESR spectra of CyDEPMPOs-OOH or CyDEPMPOs-OO*t*-Bu, respectively, representative examples being shown in Figure 4. Regarding the trapping of $O_2^{\cdot-}$ the same ESR patterns were obtained whether the radical was formed using the enzymatic hypoxanthine (HY)/xanthine oxidase (XO) system in diethylenetriaminepentaacetic acid (DTPA)-supplemented aerated phosphate buffer (pH 7.4), or by alternative methods such as KO_2/crown ether reagent in DMSO, or photolysis of 30% H_2O_2. CyDEPMPOs-OO*t*Bu adducts were easily obtained by continuous photolysis in pure *t*BuOOH. The CyDEPMPOs-OOH signal disappeared when excess superoxide dismutase (SOD) was added to the HY/XO generator, while that of CyDEPMPOs-OO*t*Bu was insensitive to the enzyme (not shown). Bubbling the system with argon prior to photolysis or after CyDEPMPOs-OOH concentration was allowed to reach a plateau (~6–10 min after addition of XO) yielded high resolution spectra (Fig. 4) which could be accurately simulated assuming a mixture of *cis*/*trans* diastereoisomers with (i) long range hyperfine coupling constants (hfcs) within the range of that reported for DEPMPO-OOR (R = H,[2,32] *t*Bu[45]) and DIPPMPO-OOH,[7] and (ii) alternate linewidth for the major species, due to an intramolecular chemical exchange between two conformers T1 and T2 in slow chemical equilibrium (Table 3). From temperature-dependent studies we have proposed that this latter unique ESR property could reflect a concerted mechanism involving rotation around the O–O bond and pseudo-rotation of the pyrrolidine ring.[46] This phenomenon leads to a non-uniform broadening of the ESR lines in the *trans* isomer causing asymmetry of the signal.[46] Modeling this conformational exchange in CyDEPMPOs-OOR (R = H, *t*Bu) at room temperature yielded mean exchange time values τ within the nanosecond scale, in the range of that previously reported in the corresponding DEPMPO peroxyl adducts.[45,46]

For Me_2CyDEPMPO-OOH we obtained a more realistic set of hfcs than that previously reported[10] and, since β-couplings follow dihedral rules, the computed ranges of a_P and $a_{H\beta}$ for T1 and T2 rotamers shown in Table 3 are characteristic of a twist $^3T_4$ or a ^3E envelope for the pyrrolidine ring, respectively.[45] For all new nitrones H_γ resolution of the minor *cis* diastereoisomer, which was not achieved in CyDEPMPOs-OOH (Fig. 4A), was only observed above 80 °C in *cis*-DEPMPO-OOH.[46] Conversely all *cis*-CyDEPMPOs-OO*t*Bu signals were fully resolved even at room temperature (Fig. 4B) contrary to *cis*-DEPMPO-OO*t*Bu.[45] For both types of peroxyl adducts there was no clear change in the stereoselectivity of the trapping reaction with the increase of the steric hindrance of the phosphoryl ligand, the largest yields in *cis* isomer being unexpectedly found for the crowded Et_2CyDEPMPO (Table 3).

Apparent half-life times ($t_{1/2app}$) of the superoxide adducts were determined from a series of repetitive acquisitions using a KO_2/18-crown-6 ether/DMSO generator in 20 mM phosphate buffer and a first-order exponential decay approximation. No significant paramagnetic byproduct was detected during the decay of CyDEPMPOs-OOH and calibration with DEPMPO gave a $t_{1/2app}$ value of 16.5 min, within the range of previous determinations.[2,6,9,41] Among the tested nitrones *trans*-MeCyDEPMPO and Me_4CyDEPMPO had the more persistent superoxide adducts, about 60% more compared to DEPMPO (Table 3).

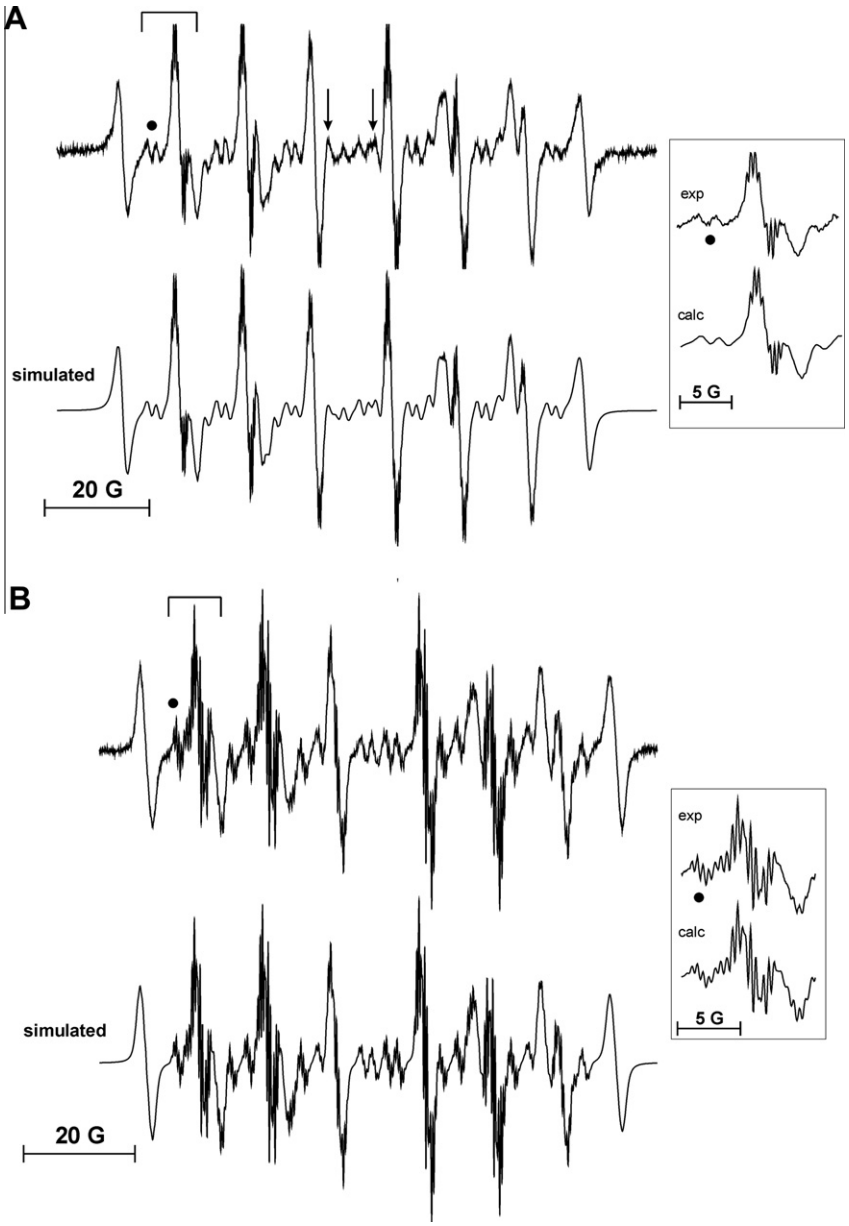

Figure 4. High resolution ESR spectra and simulations of (A) superoxide and (B) *tert*-butoxyl adducts of Et_2CyDEPMPO. Samples contained: (A) nitrone (0.1 M), hypoxanthine (0.4 mM), xanthine oxidase (0.04 units/mL), DTPA (1 mM) incubated for 6.5 min in phosphate buffer (20 mM, pH 7.4) followed by argon bubbling; (B) nitrone (0.05 M) and *t*BuOOH (10 mM) continuously UV-photolyzed in degassed anhydrous toluene. Signals were acquired at 9.79 GHz with a 100-kHz modulation frequency and 10 mW microwave power. Other acquisition parameters (A and B): sweep width (115 G, 100 G); modulation amplitude (0.16 G, 0.05 G); time constant (20.48 ms, 10.24 ms); receiver gain (6.3×10^5, 6.3×10^4), scan rate (2.7 G/s, 1.2 G/s) and number of accumulated scans (5, 1). Inserts: experimental and calculated spectra of the selected region. Arrows indicate non-composite lines of the hydroxyl radical adduct (~9% of the total signal) and (●) indicate selected lines of the *cis* adduct.

2.5. Spin trapping of H· and of C- and O-centered radicals using a primary HO· source or photolysis (Table 4)

Reduction of CyDEPMPOs by $NaBH_4$ in the presence of molecular oxygen afforded the corresponding CyDEPMPO-H nitroxides. After careful degassing of the samples, highly resolved signals were obtained showing two non-equivalent β-hydrogens and hfcs similar to that obtained in DEPMPO-H (i.e., in G): a_N = 15.31, a_P = 50.52, $a_{H\beta1}$ = 21.24, $a_{H\beta2}$ = 20.31 and $a_{H\gamma}$ = 0.33 (Me); 0.53, 0.45, 0.41, 0.19).

Other spin adducts of C-centered radicals were obtained in phosphate buffer either using excess adequate substrate in the presence of Fenton-generated HO· as a primary source, or photolytically. For methyl, 1-hydroxyethyl, $CO_2^{\cdot-}$ and *t*BuO· radical adducts, the lines were symmetric indicating the presence of one species and calculated a_P values of 45–54 G suggest a preferential pseudo-axial geometry for the C–P bond with a kinetically-favoured *trans* configuration. Stereoselective trapping of these four radicals on nitrones from the DEPMPO family has been previously reported,[2,6,7] with the exception of C_5-substituted phenyl DEPMPO which yielded *cis*/*trans* mixtures of diastereoisomers with $CO_2^{\cdot-}$ and *t*BuO having low a_P values of ~35 G, indicating a pseudo-equatorial geometry of the diethoxyphosphoryl group.[5]

When the glutathionyl radical (GS·) was generated in the presence of CyDEPMPOs all resulting ESR spectra were composed of mixtures of two nitroxides, the simulation of which gave sets of hfcs close to that of DEPMPO-SG[47] for the major species, and Me_2-CyDEPMPO-OH[10] (e.g., with a_P >50 G; see also data below) for the

Table 3
Computer simulated ESR parameters (upper part) and apparent half-life times (lower part) of superoxide and *tert*-butylperoxyl adducts of CyDEPMPOs at room temperature

Radical	hfcs (G)	CyDEPMPO		*trans*-MeCyDEPMPO[a]		*cis*-MeCyDEPMPO[a]		Me_2CyDEPMPO		Et_2CyDEPMPO		Me_4CyDEPMPO	
trans[b]-HOO·		(90%)[c]		(87%)		(96%)		(95%)		(88%)		(93%)	
		T1(45%)[d]	T2(55%)	T1(40%)	T2(60%)	T1(50%)	T2(50%)	T1(47%)	T2(53%)	T1(45%)	T2(55%)	T1(56%)	T2(44%)
		τ = 6.1[e]		τ = 5.5		τ = 6.5		τ = 19.6		τ = 6.5		τ = 5.4	
	a_N	13.2	13.0	12.6	13.3	12.9	13.2	12.8	13.2	13.2	12.8	12.8	13.3
	a_P	57.0	46.4	56.7	47.1	56.9	47.0	53.9	49.5	56.9	47.3	56.6	46.6
	$a_{H\beta}$	12.8	9.0	13.1	9.2	12.9	9.0	12.1	9.7	13.0	9.1	12.3	9.0
	$a_{H\gamma}$	0.35 (Me)		0.35 (Me)		0.37 (Me)		0.33 (Me)		0.38 (Me)		0.39 (Me)	
		0.91/0.63		0.90/0.63		0.91/0.62		0.85/0.64		0.87/0.64		0.6/0.8	
		0.47/0.45		0.45/0.33		0.44/0.44		0.47/0.11		0.46/0.34		0.2	
cis-HOO·		(10%)		(13%)		(4%)		(5%)		(12%)		(7%)	
	a_N	13.4		13.4		13.5		13.4		13.4		13.6	
	a_P	40.6		40.8		39.3		40.7		40.7		43.1	
	$a_{H\beta}$	11.2		9.4		11.6		9.1		9.2		10.6	
	$a_{H\gamma}$	1.41		1.70		1.83		1.74		1.57		1.30	
trans-*t*BuOO·		(92%)[f]		(92%)		(91%)		(86%)		(88%)		(92%)	
		T1(58%)[d]	T2(42%)	T1(58%)	T2(42%)	T1(65%)	T2(35%)	T1(57%)	T2(43%)	T1(57%)	T2(43%)	T1(56%)	T2(44%)
		τ = 18		τ = 38		τ = 60		τ = 12		τ = 12		τ = 25	
	a_N	12.35	12.34	12.36	12.42	12.33	12.05	12.39	12.14	12.35	12.05	12.26	12.20
	a_P	48.09	52.27	49.75	47.84	47.59	53.09	47.64	53.20	47.66	53.15	52.83	48.15
	$a_{H\beta}$	9.28	10.53	10.37	8.57	9.11	10.55	9.13	10.57	9.14	10.55	10.16	9.23
	$a_{H\gamma}$	0.38 (Me)		0.36 (Me)		0.36 (Me)		0.36 (Me)		0.36 (Me)		0.38 (Me)	
		1.10/0.59		1.12/0.58		1.08/0.60		1.08/0.60		1.08/0.60		1.04/0.62	
		0.46/0.46		0.47/0.43		0.47/0.43		0.47/0.43		0.47/0.43		0.49/0.48	
cis-*t*BuOO·		(8%)		(8%)		(9%)		(14%)		(12%)		(8%)	
	a_N	12.75		12.77		12.70		12.82		12.76		12.81	
	a_P	39.20		37.46		40.70		37.77		37.68		40.09	
	$a_{H\beta}$	8.29		7.84		8.40		7.85		7.70		9.38	
	$a_{H\gamma}$	0.38 (Me)/		0.37 (Me)/		0.45 (Me)/		0.37 (Me)/		0.37 (Me)/		1.58	
		1.71		1.84		1.70		1.85		1.88			
		0.54/0.45		0.51/0.46/		0.50/0.30		0.51/0.46/		0.51/0.46/			
				0.15				0.16		0.16			
$t_{1/2app}$ of superoxide adduct[g] (min)		10.2		26.3		16.2		12.3		12.4		26.4	

[a] Relative position of P = O versus Me substituent of the P-containing heterocycle.
[b] *cis*/*trans* indicate the relative position of trapped radical with respect to the P-containing heterocyle.
[c] From HY/XO system in phosphate buffer (pH 7.4).
[d] T1 and T2 refer to slowly exchanging rotamers.
[e] Computed average exchange time (ns).
[f] From *t*-BuOOH/hν in degassed toluene.
[g] From KO_2/crown ether/DMSO generator in 20 mM phosphate buffer (pH 7.4).

minor species. A very good agreement with experimental signals (r >0.90) was obtained due to the distinct separation of the ESR low-field lines from each adduct, ranging 2.0–3.0 G (Fig. 5A) and we assume they are *cis*/*trans* diastereoisomers. Likewise, when the spectra were recorded using the same conditions the relative amount of the minor species decreased with increasing substitution on the dioxaphosphorinane ring, a property compatible with the formation of the *cis* diastereoisomer.

2.6. Diastereoisomery and kinetic behavior of hydroxyl radical adducts

For evaluation of HO· trapping ability and the stability of the resulting CyDEPMPOs-OH adducts we first used either a H_2O_2 (2 mM)/Fe^{2+} (1 mM)-driven Fenton reaction or UV photolysis of 1% H_2O_2 as radical producing systems. As expected from earlier results on Me_2CyDEPMPO-OH,[10] these generators yielded mixtures of *cis*/*trans* diastereoisomers having very distinct ESR signals (Fig. 5B). Even in non degassed milieu the tops of the low-field lines from the spectra of each diastereoisomer were separated by 1.5–1.9 G. This unique spectral property of CyDEPMPOs-OH allowed to perform more reliable simulations because less parameters had to be adjusted, and hfcs listed in Table 4 were then calculated from the best resolved signals recorded in deoxygenated milieu.

For each pair of diastereoisomers, couples of calculated $a_{H\beta}$ (i.e., ~14 G, 12 G) matched those we previously calculated for DEPMPO-OH and DIPPMPO-OH based on the analysis of their ESR line asymmetries[32] and, due to this similarity, we therefore assigned them to the *cis* and *trans* configurations of CyDEPMPOs-OH, respectively (Table 4). Accordingly, β-couplings values in *trans*-CyDEPMPOs-OH indicate pseudo-axial positions for both hydroxyl and phosphoryl groups, with dihedral angles lower than 18° and 30°, respectively, a geometry which should favor stabilizing anomeric interactions. Such an electronic effect may also explain the relatively high a_P values (by about 2 G compared to *trans* adducts) in most *cis*-CyDEPMPOs-OH, which nevertheless retain their β-C–H bond in a less pseudo-equatorial position, giving higher $a_{H\beta}$ couplings. From this rationale the marked lower a_P value for *cis*-M_4CyDEPMPO-OH could reflect an increased steric repulsion between –OH and –P(O) groups that force the latter to occupy a more equatorial position (Table 4).

To evaluate the usefulness of new CyDEPMPOs as tools to investigate the mechanism of hydroxyl radical adduct formation in a biological environment, we determined *cis*/*trans* ratios of CyDEPMPOs-OH using either the two above-cited generators, or two

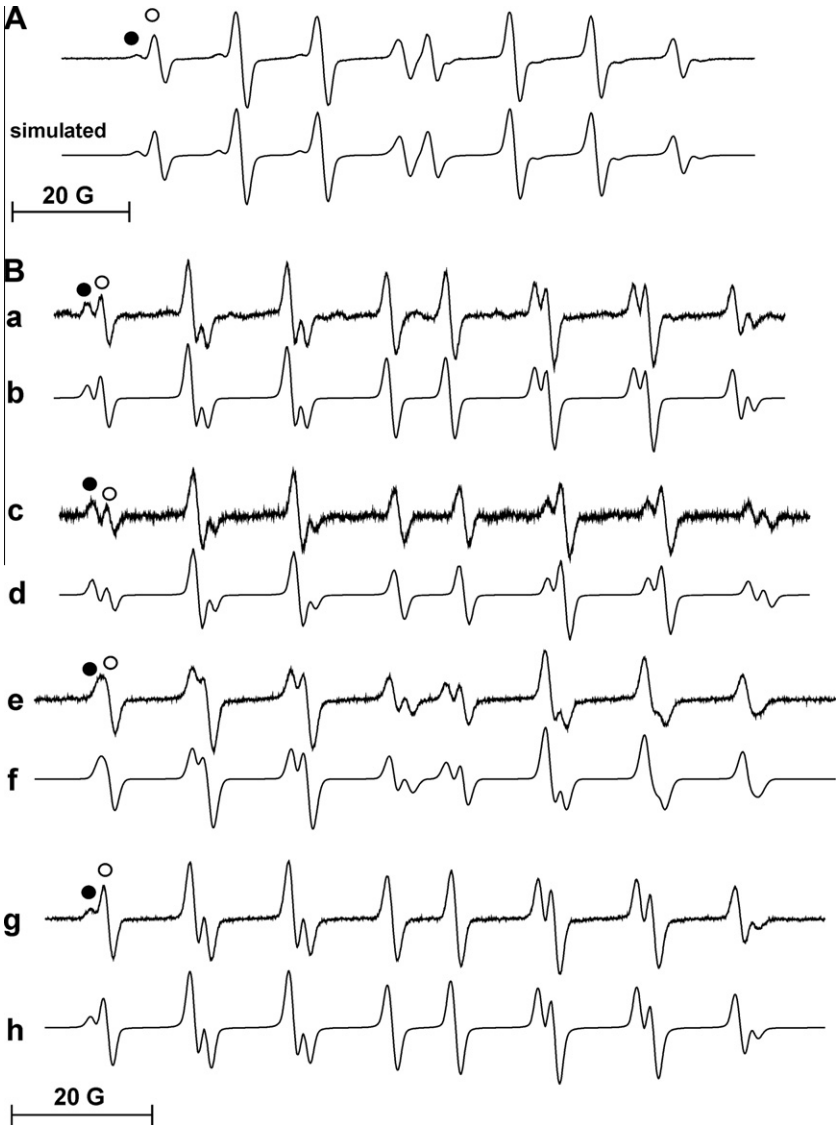

Figure 5. (A) ESR spectrum of glutathionyl radical adduct of CyDEPMPO obtained upon incubation of 0.1 M nitrone, 0.13 M GSH and a Fenton reagent consisting of 1 mM $FeSO_4$ and 1 mM H_2O_2 in 20 mM phosphate buffer. Instrument settings: microwave power, 10 mW; sweep width, 120 G; modulation amplitude, 0.07 G; time constant, 20.48 ms, receiver gain, 5×10^4 and scan rate 1.4 G/s. The low-field lines of *trans* (○) and *cis* (●; 13% of the total signal from the simulated signal shown below) diastereoisomers are shown. (B) Typical ESR spectra in 20 mM phosphate buffer (pH 7.4) of hydroxyl radical adducts of (a) CyDEPMPO (from photolysis of 1% H_2O_2); (c) Et_2CyDEPMPO (from a Fenton reaction between 1 mM $FeSO_4$ and 1 mM H_2O_2); (e) Me_4CyDEPMPO (from Fe^{3+} (1 mM)-catalyzed nucleophilic addition of water); (g) Et_2CyDEPMPO (from reduction of superoxide adduct by GSH+GPx). From simulations (b, d, f and h) of signals (a, c, e and g), respectively, the calculated percentages of *cis* (●) over *trans* (○) diastereoisomers are: 33, 51, 41, and 26, respectively. Microwave power was 10 mW throughout and other settings were (signals a/c/e/g): time constant (ms), 40.96/40.96/20.48/20.28; modulation amplitude (G), 0.05/0.12/0.05/0.5; receiver gain ($\times 10^5$), 3.2/5/1.6/1; scan rate (G/s), 1.2/0.7/1.4/2.

additional radical- and nonradical-based systems, that is, reduction of pre-formed superoxide adduct by a mixture of GPx and reduced glutathione (GSH), or nucleophilic addition of water, respectively. In order to reliably compare all nitrones experiments were performed by carefully controlling time since we have shown that diastereoisomers of DEPMPO-OH and DIPPMPO-OH have different stabilities.[32]

Briefly, in the reductive system the HY/XO superoxide generating system was run for 6 min in nitrone (0.1 M)- and DTPA (1 mM)-containing phosphate buffer (20 mM; pH 7.4), then formation of $O_2^{\cdot-}$ and its potential dismutation product (H_2O_2) was immediately stopped by adding 10 units/mL SOD and 20 units/mL catalase. Conversion of CyDEPMPOs-OOH into CyDEPMPOs-OH was then achieved by adding GSH (1.2 mM) and GPx (10 units/mL) to the mixture so that all spectral acquisitions were started 7 min after initial addition of XO. In the Fenton and photolytic systems, the spin adducts were allowed to build up for 1 min then addition of catalase (20 units/mL) or cut off of UV irradiation were performed, respectively. In these two systems spectra were recorded 1.5 min after $HO^{\cdot}$ generation. In experiments using Fe^{3+} (1 mM)-catalyzed nucleophilic addition of water, the maximal concentration of spin adduct was considered to occur immediately and ESR scan was initiated after 1 min.

The mean percentages of *cis*-CyDEPMPOs-OH along with the four generating systems are given in Table 5. Of the studied mechanisms leading to formation of the $HO^{\cdot}$ spin adduct, nucleophilic addition of water under metal ion catalysis showed the lowest stereoselectivity with little differences between nitrones. The mechanism involves the concerted formation of a metal ion complex with the negatively charged nitronyl oxygen and simultaneous nucleophilic attack of one oxygen lone pair of water on the resulting electron-poor nitronyl carbon.[31] Although it is not a radical pathway,

Table 4
Calculated ESR parameters of different radical adducts of CyDEPMPOs

Radical	hfcs (G)	CyDEPMPO		*trans*-MeCyDEPMPO		*cis*-MeCyDEPMPO		Me_2CyDEPMPO		Et_2CyDEPMPO		Me_4CyDEPMPO	
H·[a]	a_N	15.23		15.21		15.17		15.18		15.16		15.28	
	a_P	52.40		52.08		52.67		52.70		52.94		53.34	
	$a_{H\beta}$	20.89/20.53		20.91/20.46		20.97/20.34		21.00/20.36		21.06/20.26		21.17/20.17	
	$a_{H\gamma}$	0.42 (Me)		0.41 (Me)		0.40 (Me)		0.42 (Me)		0.43 (Me)		0.40 (Me)	
		0.50/0.34		0.50/0.35		0.49/0.39		0.52/0.38		0.51/0.35		0.51/0.51	
		0.33/0.18		0.32/0.18		0.34/0.18		0.30/0.19		0.32/0.18		0.32/0.18	
·CH_3[b]	a_N	15.04		15.03		15.02		14.23		14.98		14.25	
	a_P	49.44		49.01		49.89		48.15		50.00		49.22	
	$a_{H\beta}$	21.34		21.33		21.29		19.91		20.91		19.38	
·$CH(OH)CH_3$[c]	a_N	14.54		14.53		14.52		14.12		14.44		14.13	
	a_P	50.82		50.26		51.40		50.72		51.44		52.10	
	$a_{H\beta}$	20.87		20.87		20.83		20.13		20.63		19.84	
$CO_2^{\cdot-}$[d]	a_N	14.37		14.37		14.39		14.32		14.32		14.38	
	a_P	53.46		53.05		53.77		53.47		53.94		54.01	
	$a_{H\beta}$	16.76		16.80		16.82		16.73		16.60		16.72	
GS·[e]		*trans* (87%)	*cis* (13%)	*trans* (88%)	*cis* (12%)	*trans* (87%)	*cis* (13%)	*trans* (92%)	*cis* (8%)	*trans* (96%)	*cis* (4%)	*trans* (93%)	*cis* (7%)
	a_N	14.06	14.06	14.06	14.05	14.07	14.09	14.03	14.04	14.01	13.86	14.06	14.15
	a_P	47.30	51.57	46.97	50.80	47.73	52.21	47.56	51.29	47.73	53.47	48.10	52.74
	$a_{H\beta}$	14.43	16.15	14.49	15.88	14.41	16.26	14.36	16.00	14.34	14.25	13.95	15.88
*t*BuO·[f]	a_N	12.87		12.95		12.75		12.85		12.86		12.70	
	a_P	45.23		44.59		46.23		45.53		45.68		46.70	
	$a_{H\beta}$	7.99		7.90		7.88		7.97		8.07		8.04	
	$a_{H\gamma}$	0.43 (Me)		0.43 (Me)		0.45 (Me)		0.43 (Me)		0.43 (Me)		0.44 (Me)	
		1.31/0.81		1.34/0.81		1.29/0.83		1.29/0.82		1.27/0.81		1.22/0.81	
		0.28/0.22		0.29/0.22		0.32/0.22		0.28/0.23		0.32/0.23		0.26/0.19	
trans-HO·[g]	a_N	13.96		13.91		13.94		13.93		13.93		13.98	
	a_P	48.78		49.06		49.22		48.90		49.00		49.73	
	$a_{H\beta}$	12.42		12.26		12.45		12.30		12.36		11.97	
	$a_{H\gamma}$	0.37 (Me)		0.36 (Me)		0.33 (Me)		0.42 (Me)		0.38 (Me)		0.99	
		0.60/0.30		0.66/0.36		0.59/0.53		0.58/0.26		0.68/0.39			
		0.22/0.15		0.30/0.11		0.18/0.03		0.20/0.12		0.23/0.22			
cis-HO·[g]	a_N	13.98		13.90		14.03		13.93		13.98		13.98	
	a_P	50.35		50.86		51.09		50.53		50.93		48.80	
	$a_{H\beta}$	14.31		14.15		14.18		14.11		13.84		14.15	
	$a_{H\gamma}$	0.37 (Me)		0.40 (Me)		0.40 (Me)		0.42 (Me)		0.46 (Me)			
		0.72/0.55		0.50/0.37		0.53/0.47		0.72/0.48		0.59/0.34			
		0.23/0.18		0.29/0.12		0.18/0.14		0.25/019		0.27/0.08			

[a] Fenton reagent supplemented with $^aNaBH_4$ in water.
[b] 20% DMSO.
[c] 20% EtOH.
[d] 0.05 M ammonium formate.
[e] 0.13 M GSH.
[f] Photolysis of 10 mM $(t\text{BuO})_2$ in degassed toluene.
[g] Fenton reaction in degassed 20 mM phosphate buffer.

Table 5
Spin trapping of hydroxyl radical on CyDEPMPOs: comparison of the percentage[a] of the *cis* diastereoisomer as a function of the producing system and apparent half-life times of spin adducts[b]

Nitrone	Photolysis of H_2O_2	Fenton reaction	Enzymatic reduction of superoxide adduct	Nucleophilic addition	$t_{1/2app}$ (min)
CyDEPMPO	31	37	21	42	3.9
trans-MeCyDEPMPO	41	48	24	52	5.7
cis-MeCyDEPMPO	29	41	26	44	5.4
Me_2CyDEPMPO	35	42	25	43	3.8
Et_2CyDEPMPO	16	44	22	43	4.2
Me_4CyDEPMPO	19	7	11	41	11.6
DEPMPO	34[c]	35[c]	25[c]	46	9.0

[a] Extracted from computer simulations of ESR spectra recorded under time controlled conditions as described in Section 2. The data represent means of 2–3 determinations (in 20 mM phosphate buffer; pH 7.4) and are accurate within 5%.
[b] From decay curves recorded using the catalase-arrested, DTPA-free Fenton system as the radical generator.
[c] Data from Culcasi et al.[32] obtained under the same experimental conditions.

nucleophilic addition can play an important role in the study of biological spin trapping using nitrones because trace metal ions can be released from damaged cells in inflammatory conditions such as rheumatoid arthritis.[48] Since *cis*-Me_4CyDEPMPO-OH percentage for nucleophilic addition in vitro is very different from that of the other tested mechanisms (Fig. 6 and Table 5), the nitrone may be probe of biological mechanisms involving the release of metal ions.

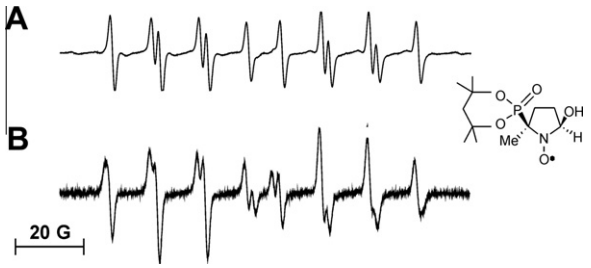

Figure 6. ESR spectra of the Me_4CyDEPMPO hydroxyl radical adduct formed by (a) a Fenton reaction (from 0.1 M nitrone, 1 mM H_2O_2 and 2 mM $FeSO_4$ in 20 mM phosphate buffer) or (b) nucleophilic synthesis (from 0.1 M nitrone and 1 mM $FeCl_3$ in water). Signals were recorded 1 min after (a) addition of excess catalase following a 3 min-incubation of the reactants, or (b) addition of iron. Computer simulations indicate that *cis*-Me_4CyDEPMPO-OH (see structure) accounts for (a) 7% and (b) 41% of the total signal with respect to the *trans* diastereoisomer, respectively.

When CyDEPMPOs-OH is the result of radical addition to the nitrone, the *cis*/*trans* ratio is a function of steric and electronic factors that drive the trapping reaction and of the relative stability of both diastereoisomers. In the DEPMPO family stereoselectivity of the spin trapping reaction is expected due to the steric hindrance of the phosphorylated versus the methyl substituent, which should favor the *trans* diastereoisomer (Fig. 2).[5,7,9] In agreement with their 'folded' crystal structure (Fig. 3), the two more bulky nitrones (namely Et_2CyDEPMPO and Me_4CyDEPMPO) yielded the lowest *cis* percentages when HO· was produced photolytically. Despite its X-ray structure, in protic solvents, due to solvation, the two faces of *cis*-MeCyDEPMPO should not be equally accessible. On the other hand, the lower stereoselectivity observed for the trapping of hydroxyl radical is in agreement with the lower steric hindrance of the trapping sites (Table 5).

In superoxide spin trapping experiments in aqueous milieu, the metal ion chelator DTPA is often introduced to prevent traces metals present in commercial phosphate buffers from catalyzing hydroxyl radical adduct formation through nucleophilic addition.[24] In our tested Fenton reagent, DTPA was omitted to be more relevant to biological conditions and because it increases the ESR linewidth.[32] Under these conditions, the data of Table 5 are characteristic of a diastereoselective trapping reaction, in line with previous results on DEPMPO.[32] According to Table 5, addition of HO· on Me_4CyDEPMPO is highly stereoselective. In vivo metal catalysts that are potential triggers of HO· formation from H_2O_2 are susceptible to chelate many biological targets including proteins, favoring a site-specific rather than a radiomimetic HO· generation.[49] Thus, differences in *cis*/*trans* ratios between the photolytical and the Fenton HO· generators in this study may be due to different iron complexing properties of the nitrones.

The *cis* percentages of CyDEPMPOs-OH in the reductive system were within the range of that of DEPMPO,[32] except for Me_4CyDEPMPO which again yielded the lowest value (Table 5). This is another advantage of this nitrone in our search for a sensitive tool to investigate bio-radical mechanisms by ESR.

The apparent half-lives of CyDEPMPOs-OH have been determined by using the DTPA-free, catalase-arrested Fenton system from 0.1 M buffered solutions of nitrones. In these conditions most hydroxyl radical adducts gave $t_{1/2app}$ values below 6 min, being significantly shorter than that of DEPMPO-OH and Me_4CyDEPMPO-OH (Table 5). Using the reductive system we reported an apparent half-life of ~7.5 min for DEPMPO-OH.[32]

3. Conclusions

Our interest in the development of spin traps that can give insights on the formation of hydroxyl radical adducts in biological systems under oxidative stress led us to synthesize a series of new DEPMPO derivatives containing a 2-oxo-1,3,2-dioxaphosphorinane ring. All prepared CyDEPMPOs nitrones were isolated and characterized as stable crystals, and their low toxicities on cultured murine fibroblasts should be compatible with biological spin trapping. We have recently proposed that valuable mechanistic information would be gained from the determination of relative *cis*/*trans* content of hydroxyl radical spin adducts provided each diastereoisomer will have distinct ESR lines.[32] All tested CyDEPMPOs meet this claim in vitro, that is, the diastereoisomeric ratios were significantly different using biologically-relevant pathways of hydroxyl radical adduct formation. Importantly, synthesized CyDEPMPOs were of different lipophilicities compared to DEPMPO and also yielded relatively persistent superoxide spin adducts. We believe CyDEPMPOs represent a fruitful class of spin traps to investigate free radical generation in vivo.

4. Experimental

4.1. Reagents and analytical instrumentation

Nuclear magnetic resonance (^{1}H NMR at 300.1 MHz, ^{13}C NMR at 75.5 MHz and ^{31}P NMR at 121.5 MHz) spectra were recorded using a Bruker AVL 300 spectrometer. Chemical shifts are expressed in δ ppm relative to internal tetramethyl silane (^{1}H and ^{13}C) or external 85% H_3PO_4 (^{31}P) and coupling constants *J* are given in Hertz. The abbreviations s, d, t, m and q refer to singlet, doublet, triplet, multiplet and quartet signal, respectively. Melting points were determined using a B-540 Buchi apparatus and are uncorrected. Elemental analyses were performed using a Thermo Finnigan EA-1112 analyzer and were within 0.2% of the theoretical values. Column chromatography was performed on Merck Silica Gel 60 (230–400 mesh). Spectrophotometrical measurements were performed on a Saphas UVmc^2 spectrophotometer (Monaco). Solvents and reagents were of the highest grade available from commercial suppliers and were used without further purification except for 2-methyl-1-pyrroline (from Acros Organics, Halluin, France) which was distilled under reduced pressure (20 mm Hg, bp: 50 °C) prior to use. Commercial diols used in the syntheses of phosphites **2a**–**2e** were 1,3-propanediol (**1a**), 2-methyl-1,3-propanediol (**1b**), 2,2-dimethyl-1,3-propanediol (**1c**), 2,2-diethylpropane-1,3-diol (**1d**) and 2,4-dimethylpentane-2,4-diol (**1e**). The nitrones DEPMPO,[35] DIPPMPO[7] and EMPO[3] were synthesized and purified as previously described. PBN was purchased from Sigma–Aldrich (Saint-Quentin Fallavier, France). Medium and reagents used in cell culture were from Life Technologies Inc. (Gaithersburg, MD, USA).

4.2. Synthesis

4.2.1. Synthesis of phosphites 2a–2e

Water (540 mg, 30.6 mmol) was added to HMPT (5 g, 30.6 mmol) in 50 mL refluxing anhydrous THF under N_2 atmosphere. The mixture was stirred at reflux for 2 h and 30.6 mmol of the corresponding diol (**1a**–**1e**) in 20 mL of dry THF was added dropwise. After 2 h reflux, the mixture was concentrated under reduced pressure to give the corresponding cyclic phosphite (**2a**–**2e**), the purity of which was found to be >95% by ^{31}P NMR, with δ values (in $CDCl_3$) in agreement with literature data: 3.47 (**2a**),[50] 3.21 (**2c**)[51] and 4.28 (**2d**).[52] Other non-reported ^{31}P NMR δ values in $CDCl_3$ were: 3.97 (**2e**) and 2.16 and 2.98 for *trans* and *cis* isomers of 5-methyl-2-oxo-1,3,2-dioxaphosphorinane (**2b**), respectively (see assignment in Section 2).

4.2.2. Synthesis of aminophosphonates 3a–3e

A mixture of 2-methyl-1-pyrroline (2.8 g, 33.7 mmol) and the corresponding cyclic phosphite **2a**–**2e** (30.6 mmol) were stirred

in toluene (5 mL) for 4–6 h at room temperature (conversion was checked by TLC or ^{31}P NMR), the mixture was poured into 30 mL water, slowly acidified to pH 3 with 11 N HCl then quickly extracted with *tert*-butyl methyl ether (TBME) (3 × 20 mL). The aqueous phase was basified to pH 9–10 with NaOH pellets then extracted with CH_2Cl_2 (4 × 20 mL). The combined organic phases were dried over $MgSO_4$, filtered and roto-evaporated to give the crude aminophosphonates **3a**–**3e** as white powders which were then purified by SiO_2 column chromatography with eluent CH_2Cl_2/EtOH 8/1.

4.2.2.1. 2-Methyl-2-(2-oxo-1,3,2-dioxaphosphinan-2-yl)pyrrolidine (3a). White crystals. Yield: 52%. Mp 79 °C. ^{31}P NMR ($CDCl_3$) δ 26.00; ^{1}H NMR ($CDCl_3$) δ 1.39 (d, J = 15 Hz, 3H, 2-Me), 1.61–2.10 (m, 6H, CH_2–CH_2–CH_2, 3-H, 4-H, NH), 2.21–2.33 (m, 1H, 3-H), 2.85–2.93 (m, 1H, 5-H), 3.05–3.11 (m, 1H, 5-H), 4.42–4.54 (m, 4H, OCH_2–CH_2–CH_2O); ^{13}C NMR ($CDCl_3$) δ 24.24 (d, J = 6.8 Hz, 2-Me), 25.90 (d, J = 3.8 Hz, 4-C), 26.76 (d, J = 8.3 Hz, CH_2–CH_2–CH_2), 34.77 (d, J = 3.8 Hz, 3-C), 47.35 (d, J = 3.8 Hz, 5-C), 60.38 (d, J = 163.8 Hz, 2-C), 67.30 (d, J = 8.3 Hz, CH_2–CH_2–CH_2), 67.40 (d, J = 8.3 Hz, CH_2–CH_2–CH_2); Anal. Calcd for $C_8H_{20}NO_3P$: C, 46.83; H, 7.86; N, 6.83. Found: C, 46.33; H, 7.83; N, 6.86.

4.2.2.2. *trans*-2-Methyl-2-(5-methyl-2-oxo-1,3,2-dioxaphosphinan-2-yl)pyrrolidine (*trans*-3b). White crystals. Yield: 55%. Mp 91 °C. ^{31}P NMR ($CDCl_3$) δ 23.25; ^{1}H NMR ($CDCl_3$) δ 0.88 (d, J = 6 Hz, 3H, CHCH_3), 1.40 (d, J = 15 Hz, 3H, 2-Me), 1.62–1.90 (m, 4H, 3-H, 4-H, NH), 2.22–2.32 (m, 1H, 3-H), 2.40–2.50 (m, 1H, CHCH$_3$), 2.79–2.87 (m, 1H, 5-H), 3.08–3.15 (m, 1H, 5-H), 4.16–4.38 (m, 4H, OCH_2CHCH$_3$CH_2O); ^{13}C NMR ($CDCl_3$) δ 11.95 (CHCH_3), 24.31 (d, J = 6.8 Hz, 2-Me), 25.98 (d, J = 3,8 Hz, 4-C), 30.96 (d, J = 9 Hz, CHCH$_3$), 34.97 (d, J = 2.8 Hz, 3-C), 47.45 (d, J = 6.8 Hz, 5-C), 61.31 (d, J = 166.8 Hz, 2-C), 73.82 (d, J = 8.3 Hz, OCH_2), 73.96 (d, J = 7.5 Hz, OCH_2); Anal. Calcd for $C_9H_{18}NO_3P$: C, 49.31; H, 8.28; N, 6.39. Found: C, 49.33; H, 8.52; N, 6.36.

4.2.2.3. *cis*-2-Methyl-2-(5-methyl-2-oxo-1,3,2-dioxaphosphinan-2-yl)pyrrolidine (*cis*-3b). Yellow oil. Yield: 16%. ^{31}P NMR ($CDCl_3$) δ 27.7; ^{1}H NMR ($CDCl_3$) δ 0.90 (d, J = 6 Hz, 3H, CHCH_3), 1.40 (d, J = 18 Hz, 3H, 2-Me), 1.60–1.93 (m, 4H, 3-H, 4-H, NH), 2.22–2.38 (m, 2H, 3-H, CHMe), 2.94–3.01 (m, 1H, 5-H), 3.03–3.12 (m, 1H, 5-H), 4.12–4.28 (m, 4H, OCH_2CHMeCH_2O); ^{13}C NMR ($CDCl_3$) δ 11.99 (CHCH_3), 23.90 (d, J = 7.5 Hz, 2-Me), 25.56 (d, J = 5.3 Hz, 4-C), 30.91 (d, J = 9 Hz, CHCH$_3$), 34.57 (d, J = 3.8 Hz, 3-C), 47.10 (d, J = 6.8 Hz, 2H, 5-C), 59.99 (d, J = 163 Hz, 2-C), 70.80 (d, J = 6.8 Hz, OC(CH$_3$)$_2$), 70.99 (d, J = 6.8 Hz, OC(CH$_3$)$_2$); Anal. Calcd for $C_9H_{18}NO_3P$: C, 49.31; H, 8.28; N, 6.39. Found: C, 48.93; H, 8.65; N, 5.55.

4.2.2.4. 2-Methyl-2-(5,5-dimethyl-2-oxo-1,3,2-dioxaphosphinan-2-yl)pyrrolidine (3c). White crystals. Yield: 80%. Mp 110 °C. ^{31}P NMR ($CDCl_3$) δ 26.43; ^{1}H NMR ($CDCl_3$) δ 1.04 (3H, CCH_3), 1.06 (3H, CCH_3), 1.41 (d, J = 15 Hz, 3H, 2-Me), 1.61–1.94 (m, 4H, 3-H, 4-H, NH), 2.26–2.38 (m, 1H, 3-H), 2.88–2.96 (m, 1H, 5-H), 3.06–3.13 (m, 1H, 5-H), 3.98–4.19 (m, 4H, OCH_2); ^{13}C NMR ($CDCl_3$) δ 21.55 (CCH$_3$), 21.72 (CCH$_3$), 24.30 (d, J = 6.8 Hz, 2-Me), 25.80 (d, J = 4.5 Hz, 4-C), 32.75 (d, J = 6.8 Hz, C(CH$_3$)$_2$), 34.80 (d, J = 3.8 Hz, 3-C), 47.35 (d, J = 6.8 Hz, 5-C), 60.26 (d, J = 163 Hz, 2-C), 76.03 (d, J = 7.5 Hz, OCH$_2$), 76.21 (d, J = 7.5 Hz, OCH$_2$); Anal. Calcd for $C_{10}H_{20}NO_3P$: C, 43.52; H, 8.35; N, 7.25. Found: C, 42.37; H, 8.21; N, 7.39.

4.2.2.5. 2-Methyl-2-(5,5-diethyl-2-oxo-1,3,2-dioxaphosphinan-2-yl)pyrrolidine (3d). White crystals. Yield: 58%. Mp 107 °C. ^{31}P NMR ($CDCl_3$) δ 27.10; ^{1}H NMR ($CDCl_3$) δ 0.84 (t, J = 9 Hz, 6H, CH_2CH_3), 1.40 (d, J = 15 Hz, 3H, 2-Me), 1.46 (q, J = 9 Hz, 4H, CH_2CH$_3$), 1.66–1.92 (m, 4H, 3-H, 4-H, NH), 2.21–2.36 (m, 1H, 3-H), 2.85–2.97 (m, 1H, 5-H), 3.05–3.13 (m, 1H, 5-H), 4.10–4.23 (m, 4H, OCH_2); ^{13}C NMR ($CDCl_3$) δ 7.02 (CH_2CH_3), 7.11 (CH_2CH_3), 22.52 (CH_2CH$_3$), 22.99 (CH_2CH$_3$), 24.32 (d, J = 7.5 Hz, 2-Me), 25.88 (d, J = 4.5 Hz, 4-C), 34.80 (d, J = 3.8 Hz, 3-C), 37.55 (d, J = 5.3 Hz, C(CH$_3$)$_2$), 47.36 (d, J = 6.8 Hz, 5-C), 60.44 (d, J = 163.1 Hz, 2-C), 73.69 (d, J = 7.5 Hz, OCH$_2$), 73.79 (d, J = 7.5 Hz, OCH$_2$); Anal. Calcd for $C_{12}H_{24}NO_3P$: C, 55.17; H, 9.20; N, 5.36. Found: C, 55.25; H, 9.56; N, 5.28.

4.2.2.6. 2-Methyl-2-(4,4,6,6-tetramethyl-2-oxo-1,3,2-dioxaphosphinan-2-yl)pyrrolidine (3e). White crystals. Yield: 63%. Mp 93 °C. ^{31}P NMR ($CDCl_3$) δ 25.32; ^{1}H NMR ($CDCl_3$) δ 1.33 (d, J = 18 Hz, 3H, 2-Me), 1.44 (3H, CCH_3), 1.45 (3H, CCH_3), 1.59 (6H, CCH_3), 1.70–1.90 (m, 4H, 3-H, 4-H, NH), 1.97–2.13 (dd, J = 15 Hz, J = 6 Hz, 2H, C(CH$_3$)$_2$CH_2C(CH$_3$)$_2$), 2.21–2.38 (m, 1H, 3-H), 2.96–3.03 (m, 2H, 5-H); ^{13}C NMR ($CDCl_3$) δ 24.30 (d, J = 7.5 Hz, 2-Me), 25.64 (d, J = 5.3 Hz, 4-C), 30.89–31.19–31.30–31.37 (C(CH_3)$_2$-CH_2C(CH_3), 34.63 (d, J = 3.8 Hz, 3-C), 47.05 (d, J = 6.8 Hz, 2H, 5-C), 47.32 (d, J = 8.3 Hz, C(CH$_3$)$_2$CH$_2$C(CH$_3$)$_2$), 59.33 (d, J = 163.1 Hz, 2-C), 79.73 (d, J = 6.8 Hz, OCMe$_2$), 79.82 (d, J = 6.8 Hz, OCMe$_2$); Anal. Calcd for $C_{12}H_{24}NO_3P$: C, 55.16; H, 9.26; N, 5.36. Found: C, 54.77; H, 9.28; N, 5.31.

4.2.3. Synthesis of nitrones 4a–4e

To aminophosphonates **3a**–**3e** (24.5 mmol) in water (50 mL) was added at 0 °C during 48 h under stirring, 30% H_2O_2 (51.45 mmol, 4.4 mL) in presence of a catalytic amount of Na_2WO_4 (403 mg, 1.22 mmol). At the end of the addition, aqueous phase was saturated with NaCl, extracted first with TBME (2 × 50 mL) then with $CHCl_3$ (4 × 50 mL). The combined chloroform phases were dried over $MgSO_4$, filtered and concentrated under vacuum to lead to crude nitrones **4a**–**4e** that were first purified by SiO_2 column chromatography with eluent CH_2Cl_2/EtOH 7/1 then recrystallized in TBME/CH_2Cl_2. These separation and purification procedures allowed to separate *cis*/*trans* diastereoisomers of **4b**, the stereochemistry of which was determined by X-ray diffraction (see Section 2).

4.2.3.1. 2-Methyl-2-(2-oxo-1,3,2-dioxaphosphinan-2-yl)-3,4-dihydro-2*H*-pyrrole 1-oxide [CyDEPMPO (4a)]. Yellow crystals. Yield: 90%. Mp 115 °C; ^{31}P NMR ($CDCl_3$) δ 14.72; ^{1}H NMR ($CDCl_3$) δ 1.73 (d, J = 15 Hz, 3H, 2-Me), 1.82–1.89 (m, 2H, CH_2–CH_2–CH_2), 2.24–2.35 (m, 1H, 3-H), 2.56–2.80 (m, 2H, 4-H), 2.90–3.03 (m, 1H, 3-H), 4.33–4.54 (m, 3H, O–CH_2–CH_2–CH_2–O), 4.98–5.07 (m, 1H, O–CH_2–CH_2–CH_2–O), 6.92 (q, J = 3 Hz et J = 6 Hz, 1H, 5-H); ^{13}C NMR ($CDCl_3$) δ 20.61 (d, J = 1 Hz, 2-Me), 25.68 (d, J = 1 Hz, 4-C), 26.48 (d, J = 3 Hz, CH_2–CH_2–CH_2), 30.91 (3-C), 68.48 (d, J = 6.7 Hz, CH_2–CH_2–CH_2), 69.95 (d, J = 8.25 Hz, CH_2–CH_2–CH_2), 75.37 (d, J = 152.5 Hz, 2-C), 135.04 (d, J = 7.5 Hz, 5-C); Anal. Calcd for $C_8H_{14}NO_4P$: C, 43.84; H, 6.44; N, 6.39. Found: C, 43.83, H, 6.60; N, 6.38.

4.2.3.2. *trans*-2-Methyl-2-(5-methyl-2-oxo-1,3,2-dioxaphosphinan-2-yl)-3,4-dihydro-2*H*-pyrrole 1-oxide [*trans*-MeCyDEPMPO (*trans*-4b)]. Yellow crystals. Yield: 81%. Mp 120 °C. ^{31}P NMR ($CDCl_3$) δ 13.59; ^{1}H NMR ($CDCl_3$) δ 0.81 (d, J = 9 Hz, 3H, CH–CH_3), 1.74 (d, J = 15 Hz, 3H, 2-CH$_3$), 2.16–2.50 (m, 1H, 3-H), 2.48–2.60 (m, 1H, CH–CH$_3$), 2.65–2.76 (m, 2H, 4-H), 2.80–3.05 (m, 1H, 3-H), 4.07–4,14 (m, 1H, OCH_2), 4.15–4.30 (m, 2H, OCH_2), 4.70–4.78 (m, 1H, OCH_2), 6.91 (q, J = 3 Hz et J = 6 Hz, 1H, 5-H); ^{13}C NMR ($CDCl_3$) δ 10.89 (CHCH$_3$), 20.65 (d, J = 15 Hz, 2-Me), 25.66 (4-C), 30.84 (3-C), 30.95 (d, J = 10 Hz, CHCH$_3$), 73.52 (d, J = 6.5 Hz, OCH$_2$), 75.38 (d, J = 150 Hz, 2-C), 75.45 (d, J = 7.5 Hz, OCH$_2$), 134,91 (d, J = 9.0 Hz, 5-C); Anal. Calcd for $C_9H_{16}NO_4P$: C, 46.35; H, 6.92; N, 6.01. Found: C, 46.13; H, 7.13; N, 5.99.

4.2.3.3. *cis*-2-Methyl-2-(5-methyl-2-oxo-1,3,2-dioxaphosphinan-2-yl)-3,4-dihydro-2H-pyrrole 1-oxide [*cis*-MeCyDEPMPO (*cis*-4b)]. Yellow crystals. Yield: 50%. Mp 110 °C. ^{31}P NMR ($CDCl_3$) δ 15.53; ^{1}H NMR ($CDCl_3$) δ 1.08 (d, J = 12 Hz, 3H, CH–CH_3), 1.74 (d, J = 15 Hz, 3H, 2-Me), 2.05–2.17 (m, 1H, 3-H), 2.21–2.28 (m, 1H, C*H*–CH_3), 2.60–2.76 (m, 2H, 4-H), 2.88–3.05 (m, 1H, 3-H), 4.05–4,18 (m, 2H, OCH_2, OCH_2), 4.34–4.44 (m, 1H, OCH_2), 4.72–4.82 (m, 1H, OCH_2), 6,91 (q, J = 3 Hz, J = 6 Hz, 1H, 5-H); ^{13}C NMR ($CDCl_3$) δ 13.05 (CHCH_3), 20.55 (d, J = 15 Hz, 2-Me), 25.61 (4-C), 30.05 (d, J = 10 Hz, $CHCH_3$), 30.95 (3-C), 73.16 (d, J = 7.5 Hz, OCH_2), 73.86 (d, J = 7,5 Hz, OCH_2), 74.98 (d, J = 153.2 Hz, 2-C), 134,88 (d, J = 9,8 Hz, 5-C); Anal. Calcd for $C_9H_{16}NO_4P$: C, 46.35; H, 6.92; N, 6.01. Found: C, 45.84; H, 7.19; N, 5.56.

4.2.3.4. 2-Methyl-2-(5,5-dimethyl-2-oxo-1,3,2-dioxaphosphinan-2-yl)-3,4-dihydro-2H-pyrrole 1-oxide [Me$_2$CyDEPMPO (4c)]. Yellow crystals. Yield: 55%. Mp 128 °C. ^{31}P NMR ($CDCl_3$) δ 14,17; ^{1}H NMR ($CDCl_3$) δ 0.89 (s, 3H, O–CH_2–C(CH_3)$_2$–CH_2–O), 1.28 (s, 3H, O–CH_2–C(CH_3)$_2$–CH_2–O), 1.76 (d, J = 15 Hz, 3H, 2-Me), 2.00–2.14 (m, 1H, 3-H), 2.62–2.74 (m, 2H, 4-H), 2.90–3.03 (m, 1H, 3-H), 3.88–3.99 (m, 2H, O–CH_2–C(CH_3)$_2$–CH_2–O), 4.18–4.23 (dd, J = 3 Hz et J = 12 Hz, 1H, O–CH_2–CC(CH_3)$_2$–CH_2–O), 4.75–4.80 (dd, J = 3 Hz, J = 12 Hz, 1H, O–CH_2–C(CH_3)$_2$–CH_2–O), 6.91 (q, J = 3 Hz, J = 6 Hz, 1H, 5-H); ^{13}C NMR ($CDCl_3$) δ 20.00 (d, J = 16 Hz, 2-Me), 21.50 (O–CH_2–C(CH_3)$_2$–CH_2–O), 25.23 (4-C), 30.37 (3-C), 32.10 (d, J = 9 Hz, O–CH_2–C(CH_3)$_2$–CH_2–O), 74.74 (d, J = 151 Hz, 2-C), 76.97 (d, J = 7 Hz, O–CH_2–C(CH_3)$_2$–CH_2–O), 78.77 (d, J = 7 Hz, O–CH_2–C(CH_3)$_2$–CH_2–O), 134.65 (d, J = 8.25 Hz, 5-C); Anal. Calcd for $C_{10}H_{18}NO_4P$: C, 48.58; H, 7.34; N, 5.67. Found: C, 48.23; H, 7.51; N, 5.53.

4.2.3.5. 2-Methyl-2-(5,5-diethyl-2-oxo-1,3,2-dioxaphosphinan-2-yl)-3,4-dihydro-2H-pyrrole 1-oxide [Et$_2$CyDEPMPO (4d)]. Yellow crystals. Yield: 77%. Mp 96 °C. ^{31}P NMR ($CDCl_3$) δ 15.14; ^{1}H NMR ($CDCl_3$) δ 0.78 (t, J = 9 Hz, 3H, CH_2–CH_3), 0.88 (t, J = 6 Hz, 3H, CH_2–CH_3), 1.22 (q, J = 6 Hz, 2H, CH_2–CH_3), 1.72 (d, J = 15 Hz, 3H, 2-Me), 1.74 (q, J = 6 Hz, 2H, CH_2–CH_3), 2.12–2.24 (m, 1H, 3-H), 2.60–2.76 (m, 2H, 4-H), 2.90–3.03 (m, 1H, 3-H), 3.98–4.07 (m, 2H, O–CH_2), 4.18–4.23 (dd, J = 3 Hz et J = 12 Hz, 1H, O–CH_2), 4.77–4.82 (dd, J = 3 Hz et J = 12 Hz, 1H, O–CH_2), 6.91 (q, J = 3 Hz et J = 6 Hz, 1H, 5-H); ^{13}C NMR ($CDCl_3$) δ 6.80 (CH_2CH_3), 7.18 (CH_2CH_3), 20.66 (d, J = 15 Hz, 2-Me), 22.07 (CH_2CH_3), 22.64 (CH_2CH_3), 25.69 (4-C), 31.00 (3-C), 37.42 (d, J = 9 Hz, C(CH_2CH_3)$_2$), 75.42 (d, J = 149.4 Hz, 2-C), 75.08 (d, J = 7,5 Hz, O–CH_2–C(CH_3)$_2$–CH_2–O), 76.88 (d, J = 7.5 Hz, O–CH_2–C(CH_3)$_2$–CH_2–O), 134.95 (d, J = 8.3 Hz, 5-C); Anal. Calcd for $C_{12}H_{22}NO_4P$: C, 52.36; H, 8.06; N, 5.09. Found: C, 52.24; H, 8.17; N, 5.05.

4.2.3.6. 2-Methyl-2-(4,4,6,6-tetramethyl-2-oxo-1,3,2-dioxaphosphinan-2-yl)-3,4-dihydro-2H-pyrrole 1-oxide [Me$_4$CyDEPMPO (4e)]. Yellow crystals. Yield: 60%. Mp 156 °C. ^{31}P NMR ($CDCl_3$) δ 14.64; ^{1}H NMR ($CDCl_3$) δ 1.40–1.41 (d, J = 3 Hz, 3H, C–CH_3), 1.53 (d, J = 3 Hz, 3H, C–CH_3), 1.60 (d, J = 3 Hz, 6H, CCH_3–CH_2–CCH_3), 1.70 (d, J = 15 Hz, 3H, 2-Me), 1.93 (d, J = 12 Hz, 1H, C(CH_3)$_2$–CH_2–C(CH_3)$_2$), 2,00–2.10 (m, 1H, 3-H), 2.21 (d, J = 12 Hz, 1H, C(CH_3)$_2$–CH_2–C(CH_3)$_2$), 2,50–2.56 (m, 1H, 4-H), 2.62–2.74 (m, 1H, 4-H), 2.73–3.05 (m, 1H, 3-H), 6.83 (q, J = 3 Hz, J = 6 Hz, 1H, 5-H); ^{13}C NMR ($CDCl_3$) δ 20.49 (d, J = 1.5 Hz, 2-Me), 25.27 (4-C), 30.62 (d, J = 5 Hz, 1 CH_3 in C(CH_3)$_2$–CH_2–C(CH_3)$_2$), 30.92 (d, J = 5 Hz, 2CH_3 in C(CH_3)$_2$–CH_2–C(CH_3)$_2$), 31.40 (d, J = 5 Hz, 1 CH_3 in C(CH_3)$_2$–CH_2–C(CH_3)$_2$), 31.62 (d, J = 1.5 Hz, 3-C), 46.42 (d, J = 9 Hz, O–C(CH_3)$_2$–CH_2–C(CH_3)$_2$–O), 74.78 (d, J = 155.5 Hz, 2-C), 82.16 (d, J = 7.5 Hz, C(CH_3)$_2$), 82.42 (d, J = 7.5 Hz, C(CH_3)$_2$), 133.94 (d, J = 8 Hz, 5-C); Anal. Calcd for $C_{12}H_{22}NO_4P$: C, 52.36; H, 8.06; N, 5.09. Found: C, 51.98; H, 8.22; N, 5.04.

4.3. X-ray diffraction analysis

Samples of nitrones recrystallized as described above were washed with cold TBME and dried under vacuum to give single crystals suitable for X-ray diffraction studies. The intensities were collected at 293 K on a Bruker-Nonius Kappa CCD diffractometer using graphite-monochromated Mo Kα radiation (λ = 0.71073 Å). Kappa CCD[53] program was used for data collection. The crystal structures were solved by direct methods[54] and all non-hydrogen atoms were refined anisotropically by full-matrix least-squares calculations based on F^2.[54] The structure resolution computing was SIR-92.[55]

Crystal data for *cis*-**4b**: M = 233.20, triclinic, Pc, a = 6.4636(2) Å, b = 6.9938(2) Å, c = 12.4669(5) Å, α = 87.9420(1)°, β = 77.9340(1)°, γ = 77.9070(3)°, V = 538.87(3) Å^3, Z = 2, space group $P\bar{1}$, ρ = 1.437 g/cm^3, μ = 2.50 cm^{-1}, 3873 reflections measured in the 1.67–25.94° θ range (1956 independent, R_{int} = 0.029).

Crystal data for **4d**: M = 275.28, monoclinic, Pc, a = 6.5915(2) Å, b = 10.0296(3) Å, c = 20.9770(8) Å, β = 91.161(1)°, V = 1386.51(8) Å^3, Z = 4, space group $P2_1/n$, ρ = 1.319 g/cm^3, μ = 2.05 mm^{-1}, 11091 reflections measured in the 3.22–28.12° θ range (3278 independent, R_{int} = 0.067).

Crystal data for **4e**: M = 275.28, orthorhombic, Pc, a = 12.6103(2) Å, b = 14.0468(3) Å, c = 16.1676(2) Å, V = 2863.84(8) Å^3, Z = 8, space group $Pbca$, ρ = 1.277 g/cm^3, μ = 1.99 cm^{-1}, 20423 reflections measured in the 2.51–25.97° θ range (2742 independent, R_{int} = 0.042).

Supplementary crystallographic data for the structures in this paper have been deposited with the Cambridge Crystallographic Data Centre as publication numbers CCDC 793305, 793307, 793315, 793316 and 793317. Copies of the data can be obtained free of charge, on application to CCDC, 12 Union Road, Cambridge CB2 1EZ, UK (fax: +44 1223 336033; E-mail: deposit@ccdc.cam.ac.uk).

4.4. Partition coefficient *P*

P values were determined using a variation of a previously reported method.[56] Briefly, 1-octanol-saturated water was obtained by strongly stirring an equal volume of distilled water and 1-octanol for 1 h at 37 °C, followed by centrifugation (5000 rpm) of the resulting aqueous layer for 10 min at 10 °C. The resulting homogenous solution was used as a solvent to prepare a stock solution of each nitrone (typically 20 mg in 10 mL) and to establish a calibration curve from the measurement of the absorbance at 234 nm of successive dilutions (up to 0.2 mM). For determination of *P* values, a 1-octanol (10 mL)/water (10 mL) solution was prepared and processed as described above where 10 mM nitrone was previously dissolved in the water portion. A 100-μL aliquot of the recovered aqueous phase was then diluted 100 times, its absorbance at 234 nm determined and *P* was calculated from the correponding calibration curve as the ratio of the nitrone concentration in 1-octanol to that in water with the following equation: $P = [\text{nitrone}]_{1\text{-octanol}}/[\text{nitrone}]_{\text{water}}$. *P* values are means at least three measurements.

4.5. Cell culture and cytotoxicity assays

3T3 murine fibroblasts (ATCC-LGC Promochem, Molsheim, France) were cultured in DMEM supplemented with 1% glucose, 10% fetal calf serum, 100 units/mL penicillin and 100 μg/mL streptomycin at 37 °C in a 5% CO_2 incubator. Cells were plated in 24-well dishes and medium was replenished every 2–3 days until confluency as previously described.[57]

In cytotoxicity studies cell necrosis was evaluated by the amount of lactate dehydrogenase (LDH) release. Aqueous stock solutions of nitrones (0.3–0.8 M) were freshly prepared and aliquots were added into each culture well of confluent cells previously

filled with phenol red-free DMEM containing 1% glucose, to reach a final volume of 0.5 mL/well. The final mixtures, which contained 0.5–100 mM of each tested nitrone, were then incubated for 3–24 h (37 °C, 5% CO_2 humidity) and the supernatants were sampled for LDH assay using a detection kit (Biolabo, Maizy, France) according to the manufacturer's protocol, with light absorption being measured at 340 nm. Data are expressed as UI/L and are representative of 6–12 independent experiments made in duplicate. Untreated controls represent wells being incubated in DMEM alone for the same period. After 24 h spin trap exposure, cells were incubated for 2 h in serum-free medium containing neutral red (50 μg/mL). The determination of cell number neutral red uptake was then obtained by monitoring the absorption difference between 560 and 620 nm using a microplate reader.[58] Medium lethal dose (LD_{50}) was determined as the spin trap concentration inducing 50% cell death and is expressed in mM from triplicate experiments. When appropriate, the concentration reducing the viability by 10% (LD_{10}) was determined from the dose–response curve.

4.6. Statistics

Biological values are expressed as mean ± SD. Differences were analyzed using a one-way ANOVA followed by a a posteriori Newman–Keuls. Intergroup differences were considered to be significant at $p < 0.05$.

4.7. Free radical generators, HO· diastereoisomers assessment and kinetics of spin adducts

Superoxide was produced at room temperature by incubating the nitrone (0.1–0.15 M) in 20 mM phosphate buffer (pH 7.4) either with a mixture of 0.4 mM HY, 0.04–0.05 units/mL XO and 1 mM DTPA, or with 18-crown-6 ether (10 mM)-solubilized KO_2 (10 mM) in DMSO.

To generate CyDEPMPOs-OH adducts at room temperature from the parent nitrone (0.05–0.1 M) four methods were alternatively used: (i) reduction of preformed CyDEPMPO-OOH in 20 mM phosphate buffer (as described above) by a mixture of GPx and GSH, as detailed in;[32] (ii) incubation with a Fenton reagent consisting of 1 mM $FeSO_4$ and 2 mM H_2O_2 in 20 mM phosphate buffer; (iii) photolysis 1% H_2O_2 in degassed phosphate buffer; (iv) incubation with 1 mM $FeCl_3$ in water.

The CyDEPMPOs adducts of $CH_3^{\cdot}$, $CH_3{}^{\cdot}CHOH$, $GS^{\cdot}$ and $CO_2^{\cdot-}$ were produced in 20 mM phosphate buffer by incubating the parent nitrone (0.05 M) with a mixture of the Fenton reagent described above and the precursor (0.05–0.2 M) DMSO, ethanol, GSH and $NaHCO_2$, respectively. CyDEPMPOs-H adduct was prepared by aerial oxidation of a mixture of aqueous nitrone (0.1 M) and ~5 mg of $NaBH_4$. CyDEPMPOs-O*t*Bu and CyDEPMPOs-OO*t*Bu adducts were obtained in degassed anhydrous toluene by continuous UV photolysis of the parent nitrone (0.05 M) with 10 mM $(tBuO)_2$ or *t*BuOOH, respectively.

The *cis*/*trans* ratios of CyDEPMPOs-OH adducts were determined for each of the four HO· generators described above by computer analyzing the ESR spectra obtained immediately after spin adduct formation was considered over, that is, after cut-off of the UV lamp or addition of Fe^{3+} in the case of H_2O_2 photolysis or nucleophilic addition of water, respectively, or after complete removal of the spin adduct precursor, that is, $O_2^{\cdot-}$ (by excess SOD+catalase) and H_2O_2 (by excess catalase alone) for the reduction of CyDEPMPOs-OOH or the Fenton reaction, respectively. To minimize simulation errors due to fitting of the linewidths the hfcs reported in Table 4 for diastereoisomers of CyDEPMPOs-OH were set as non-variable parameters.

The kinetic parameters of CyDEPMPOs-OOH and CyDEPMPOs-OH adducts were extracted from decay curves constructed by timely monitoring ESR spectra recorded using the KO_2-driven or catalase-stopped Fenton systems described above, respectively. For both types of spin adducts a first-order exponential decay approximation was performed to determine $t_{1/2app}$ values using GraphPad Prism software. Data are means of at least three determinations, with 5–10% accuracy.

4.8. ESR spectroscopy

Throughout the study, the same 10-mm quartz flat cell was used and all procedures allowing to acquire ESR signals under the strictly controlled time conditions have been described elsewhere.[32] X-band (9.78 GHz) ESR spectra were recorded at room temperature with Bruker spectrometers (ESP 300 or EMX) with 100 kHz modulation frequency and 10 mW microwave power. Other instrument settings in individual experiments are given in the legends of Figures. Splitting parameters were obtained from computer simulations of the best resolved signals using the program of Rockenbauer and Korecz.[59]

Acknowledgments

We thank M. Giorgi for his kind help in collection of crystallographic data. This study was supported and by the Agence Nationale pour la Recherche (ANR-09-BLAN-0005-03-ROS SIGNAL).

References and notes

1. Harbour, J. R.; Chow, V.; Bolton, J. R. *Can. J. Chem.* **1974**, *52*, 3549.
2. Fréjaville, C.; Karoui, H.; Tuccio, B.; Le Moigne, F.; Culcasi, M.; Pietri, S.; Lauricella, R.; Tordo, P. *J. Med. Chem.* **1995**, *38*, 258.
3. Olive, G.; Mercier, A.; Le Moigne, F.; Rockenbauer, A.; Tordo, P. *Free Radical Biol. Med.* **2000**, *28*, 403.
4. Villamena, F. A.; Rockenbauer, A.; Gallucci, J.; Velayutham, M.; Hadad, C. M.; Zweier, J. L. *J. Org. Chem.* **2004**, *69*, 7994.
5. Karoui, H.; Nsanzumuhire, C.; Le Moigne, F.; Tordo, P. *J. Org. Chem.* **1999**, *64*, 1471.
6. Stolze, K.; Udilova, N.; Nohl, H. *Free Radical Biol. Med.* **2000**, *29*, 1005.
7. Chalier, F.; Tordo, P. *J. Chem. Soc., Perkin Trans. 2* **2002**, 2110.
8. Xu, Y. K.; Chen, Z. W.; Sun, J.; Liu, K.; Chen, W.; Shi, W.; Wang, H. M.; Liu, Y. *J. Org. Chem.* **2002**, *67*, 7624.
9. Hardy, M.; Chalier, F.; Finet, J. P.; Rockenbauer, A.; Tordo, P. *J. Org. Chem.* **2005**, *70*, 2135.
10. Kamibayashi, M.; Oowada, S.; Kameda, H.; Okada, T.; Inanami, O.; Ohta, S.; Ozawa, T.; Makino, K.; Kotake, Y. *Free Radical Res.* **2006**, *40*, 1166.
11. Hardy, M.; Rockenbauer, A.; Vásquez-Vivar, J.; Felix, C.; Lopez, M.; Srinivasan, S.; Avadhani, N.; Tordo, P.; Kalyanaraman, B. *Chem. Res. Toxicol.* **2007**, *20*, 1053.
12. Chalier, F.; Hardy, M.; Ouari, O.; Rockenbauer, A.; Tordo, P. *J. Org. Chem.* **2007**, *72*, 7886.
13. Hardy, M.; Bardelang, D.; Karoui, H.; Rockenbauer, A.; Finet, J. P.; Jicsinszky, L.; Rosas, R.; Ouari, O.; Tordo, P. *Chem. Eur. J.* **2009**, *15*, 11114.
14. Zhao, H.; Joseph, J.; Zhang, H.; Karoui, H.; Kalyanaraman, B. *Free Radical Biol. Med.* **2001**, *31*, 599.
15. Tsai, P.; Ichikawa, K.; Mailer, C.; Pou, S.; Halpern, H. J.; Robinson, B. H.; Nielsen, R.; Rosen, G. M. *J. Org. Chem.* **2003**, *68*, 7811.
16. Stolze, K.; Udilova, N.; Rosenau, T.; Hofinger, A.; Nohl, H. *Biol. Chem.* **2003**, *384*, 493.
17. Stolze, K.; Udilova, N.; Rosenau, T.; Hofinger, A.; Nohl, H. *Biochem. Pharmacol.* **2005**, *69*, 297.
18. Stolze, K.; Rohr-Udilova, N.; Rosenau, T.; Stadtmüller, R.; Nohl, H. *Biochem. Pharmacol.* **2005**, *69*, 1351.
19. Stolze, K.; Rohr-Udilova, N.; Rosenau, T.; Hofinger, A.; Kolarich, D.; Nohl, H. *Bioorg. Med. Chem.* **2006**, *14*, 3368.
20. Stolze, K.; Rohr-Udilova, N.; Rosenau, T.; Hofinger, A.; Nohl, H. *Bioorg. Med. Chem.* **2007**, *15*, 2827.
21. Xu, Y.; Kalyanaraman, B. *Free Radical Res.* **2007**, *41*, 1.
22. Stolze, K.; Rohr-Udilova, N.; Hofinger, A.; Rosenau, T. *Bioorg. Med. Chem.* **2008**, *16*, 8082.
23. Stolze, K.; Rohr-Udilova, N.; Hofinger, A.; Rosenau, T. *Bioorg. Med. Chem.* **2009**, *17*, 7572.
24. Buettner, G. R.; Oberley, L. W. *Biochem. Biophys. Res. Commun.* **1978**, *83*, 69.
25. Shi, H.; Timmins, G.; Monske, M.; Burdick, A.; Kalyanaraman, B.; Liu, Y.; Clément, J. L.; Burchiel, S.; Liu, K. J. *Arch. Biochem. Biophys.* **2005**, *437*, 59.
26. Chen, Y. R.; Chen, C. L.; Yeh, A.; Liu, X.; Zweier, J. L. *J. Biol. Chem.* **2006**, *281*, 13159.
27. Karoui, H.; Rockenbauer, A.; Pietri, S.; Tordo, P. *Chem. Commun.* **2002**, 3030.

28. Bardelang, D.; Rockenbauer, A.; Karoui, H.; Finet, J. P.; Biskupska, I.; Banaszak, K.; Tordo, P. *Org. Biomol. Chem.* **2006**, *4*, 2874.
29. Han, Y.; Tuccio, B.; Lauricella, R.; Villamena, F. A. *J. Org. Chem.* **2008**, *73*, 7108.
30. Han, Y.; Liu, Y.; Rockenbauer, A.; Zweier, J. L.; Durand, G.; Villamena, F. A. *J. Org. Chem.* **2009**, *74*, 5369.
31. Makino, K.; Hagiwara, T.; Hagi, A.; Nishi, M.; Murakami, A. *Biochem. Biophys. Res. Commun.* **1990**, *172*, 1073.
32. Culcasi, M.; Rockenbauer, A.; Mercier, A.; Clément, J. L.; Pietri, S. *Free Radical Biol. Med.* **2006**, *40*, 1524.
33. Page, P.; Mazières, M. R.; Bellan, J.; Sanchez, M. *Phosphorus, Sulfur Silicon Relat. Elem.* **1992**, *70*, 205.
34. Mosbo, J. A.; Verkade, J. G. *J. Am. Chem. Soc.* **1973**, *95*, 204.
35. Barbati, S.; Clément, J. L.; Fréjaville, C.; Bouteiller, J. C.; Michel, J. C.; Yadan, J. C.; Tordo, P. *Synthesis* **1999**, 2036.
36. Murahashi, S. I.; Mitsui, H.; Shiota, T.; Tsuda, T.; Watanabe, S. *J. Org. Chem.* **1990**, *55*, 1736.
37. Farrugia, L. J. *J. Appl. Crystallogr.* **1997**, *30*, 565.
38. Cova, D.; De Angelis, L.; Monti, E.; Piccinini, F. *Free Radical Res. Commun.* **1992**, *15*, 353.
39. Haseloff, R. F.; Mertsch, K.; Rohde, E.; Baeger, I.; Grigor'ev, I. A.; Blasig, I. E. *FEBS Lett.* **1997**, *418*, 73.
40. Arakaki, N.; Kajihara, T.; Arakaki, R.; Ohnishi, T.; Kazi, J. A.; Nakashima, H.; Daikuhara, Y. *J. Biol. Chem.* **1999**, *274*, 13541.
41. Rohr-Udilova, N.; Stolze, K.; Marian, B.; Nohl, H. *Bioorg. Med. Chem. Lett.* **2006**, *16*, 541.
42. Rohr-Udilova, N.; Stolze, K.; Sagmeister, S.; Parzefall, W.; Marian, B.; Nohl, H.; Schulte-Hermann, R.; Grasl-Kraupp, B. *Bioorg. Med. Chem. Lett.* **2007**, *17*, 5698.
43. Pietri, S.; Liebgott, T.; Fréjaville, C.; Tordo, P.; Culcasi, M. *Eur. J. Biochem.* **1998**, *254*, 256.
44. Cruz-Gregorio, S.; Rodriguez-Palacios, V.; Höpfl, H.; Quintero, L.; Sartillo-Piscil, F. *J. Org. Chem.* **2009**, *74*, 197.
45. Clément, J. L.; Finet, J. P.; Fréjaville, C.; Tordo, P. *Org. Biomol. Chem.* **2003**, *1*, 1591.
46. Rockenbauer, A.; Clément, J. L.; Culcasi, M.; Mercier, A.; Tordo, P.; Pietri, S. *J. Phys. Chem. A* **2007**, *111*, 4950.
47. Karoui, H.; Hogg, N.; Fréjaville, C.; Tordo, P.; Kalyanaraaman, B. *J. Biol. Chem.* **1996**, *271*, 6000.
48. Morris, C. J.; Earl, J. R.; Trenam, C. W.; Blake, D. R. *Int. J. Cell Biol.* **1995**, *27*, 109.
49. Halliwell, B.; Gutteridge, J. M. C. *Arch. Biochem. Biophys.* **1986**, *246*, 501.
50. Klosinski, P. *Tetrahedron Lett.* **1990**, *31*, 2025.
51. Maffei, M.; Buono, G. *Tetrahedron* **2003**, *59*, 8821.
52. Satish Kumar, N. S.; Kumaraswamy, S.; Said, M. A.; Kumara Swamy, K. C. *Org. Process Res. Dev.* **2003**, *7*, 925.
53. Nonius, B. V. Kappa CCD Reference Manual; PO Box 811, 2600 Av. Delft, The Netherlands, 1998.
54. Sheldrick, G. M. *Acta Crystallogr., Sect. A* **2008**, *64*, 112.
55. Almatore, A.; Cascarano, G.; Giocovazzo, C.; Guagliardi, A.; Burla, M. C.; Polidori, G.; Camalli, M. *J. Appl. Crystallogr.* **1994**, *27*, 435.
56. Janzen, E. G.; West, M. S.; Kotake, Y.; DuBose, C. M. *J. Biochem. Biophys. Methods* **1996**, *32*, 183.
57. Culcasi, M.; Muller, A.; Mercier, A.; Clément, J. L.; Payet, O.; Rockenbauer, A.; Marchand, V.; Pietri, S. *Chem. Biol. Interact.* **2006**, *164*, 215.
58. Borenfreund, E.; Puerner, J. A. *Toxicol. Lett.* **1985**, *24*, 119.
59. Rockenbauer, A.; Korecz, L. *Appl. Magn. Reson.* **1996**, *10*, 29.